17th World Conference on Earthquake Engineering, 17WCEE
Sendai, Japan - September 13th to 18th 2020

DYNAMIC RUPTURE SIMULATION OF THE 2016 KUMAMOTO, JAPAN, EARTHQUAKE SEQUENCE

H. Si [(1)], S. Kumagai [(2)], and Y. Yuzawa [(3)]

[(1)] *Principal researcher, Seismological Research Institute Inc., shj@seismo-r.com*
[(2)] *Chief, Tohoku-Electric Power Co., Inc., kumagai.shuji.ea@tohoku-epco.co.jp*
[(3)] *Group Manager, Tokyo Electric Power Services Co., Ltd., yyuzawa@tepsco.co.jp*

…

Abstract

The 2016 Kumamoto, Japan, earthquake sequence mainly consists of an M_w 6.2 earthquake happened at 21:26 Japan Standard Time (JST) on April 14, 2016, followed 28 hours later by an M_w 7.0 earthquake. Both the earthquakes struck the Kumamoto prefecture with a maximum seismic intensity of 7 on the Japan Meteorological Agency (JMA) and caused heavy casualty and economic loss. The M_w 6.2 earthquake ruptured only Hinagu fault (HF), and M_w 7.0 earthquake ruptured both the Hinagu fault and the adjacent Futagawa fault. In this study, we try to simulate the rupture process of these two earthquakes and the ground motions from the M_w 7.0 earthquake.

We adopted a curved grid finite difference method (CG-FDM) [1][2] for the simulation since the method can model the complicated fault geometry for the M_w 7.0 earthquake and the seismic-wave propagation in 3D heterogeneous media. We modelled the M_w 7.0 earthquake on a smoothed non-planar fault plane based on the surface rupture trace, and also modelled the M_w 6.2 earthquake on a higher dip angle planar fault plane located in the northern part of Hinagu fault (HF). The fault planes are embedded within a 3D heterogeneous media based on the Japan integrated velocity structure model (JIVSM) proposed by Koketsu et al. (2008, 2012) [3][4]. The tectonic stress subjected to the models is estimated based on the model proposed by Yoshida et al. (2016) [5]. The dynamic friction coefficients, critical distance and the other parameters are also assumed refer to the past studies.

We performed the simultaneous dynamic rupture simulations both for the M_w 7.0 earthquake and the M_w 6.2 foreshock. For the M_w 7.0 earthquake, the rupture started from the segment of Hinagu fault (HF) and successfully propagated to the Futagawa fault (FF). For the foreshock, however, the rupture stopped on Hinagu fault (HF) and haven't propagate to the Futagawa fault (FF). The results reproduced the real rupture sequence observed during the 2016 Kumamoto earthquakes. We also confirmed that the synthetic waveforms are generally consistent with the observed ones in the main features.

Keywords: 2016 Kumamoto earthquake sequence; Ground motion; Dynamic rupture simulation; CG-FDM

1. Introduction

The 2016 Kumamoto, Japan, earthquake sequence mainly consists of an M_w 6.2 earthquake happened at 21:26 Japan Standard Time (JST) on April 14, 2016, followed 28 hours later by an M_w 7.0 earthquake. Both the earthquakes struck the Kumamoto prefecture with a maximum seismic intensity of 7 on the Japan Meteorological Agency (JMA) and caused heavy casualty and economic loss. The M_w 6.2 earthquake ruptured only Hinagu fault (HF), and M_w 7.0 earthquake ruptured both the Hinagu fault and the adjacent Futagawa fault (FF). Though both the two earthquakes nucleated on the adjacent points on the northern parts of the Hinagu fault, the consequence of the two earthquakes are quite different. In this study, we try to simulate the rupture process of these two earthquakes and try to understand the reason that the foreshock rupture could not propagate to the Futagawa fault.

2. Method and Fault Model

We use the curved grid finite difference method (CG-FDM, Zhang et al., 2014, 2016) [1][2] to model the spontaneous dynamic rupture of the 2016 Kumamoto earthquake sequence. According to [1], the method can model the rupture dynamics of a fault with complex geometry in 3D media with irregular topography by using general curvilinear grids. In the calculation, the method solves first order stress-velocity formulation of the elastodynamic equations in curvilinear coordinates, using perfectly matched layer (PML) to absorb outgoing wave at the truncated boundaries except at the free surface. The method uses collocated grid for FDM, that all the parameters are located in the same grid point. Split nodes are used to represent the fault. The slip-weakening law is used. No inelastic attenuation is considered in the method. The method has been validated by the benchmark models organized by Southern California Earthquake Center (SCEC, Harris et al., 2018[6]).

Fig. 1 illustrates the traces of the surface faults ruptured during the mainshock of Kumamoto earthquake based on the results investigated by Shirahama et al. (2016) [7], which extends to about 50 km in the strike direction. We model the fault model for the mainshock with a simplified and smoothed surface trace from the surface breaks by Shirahama et al. (2016) [7]. Fig.1 (middle) shows the surface trace of the fault model used in the calculation. The total length and width of the fault model is 51 km and 18 km, respectively. We embedded the fault model within a heterogeneous media proposed by Koketsu et al. (2008, 2012) [3][4] shown in Fig. 1 (right). Referring to the rupture model estimated by the waveform inversion (e.g., Kobayashi et al., 2017 [8]), the dip angle of the fault model is set to 75 degree. A bird view of the fault model for mainshock used in this study is shown in Fig.2 (left).

For the fore shock occurred on 14 Apr. 2016, the fault is on the northern part of Hinagu fault and on a short subparallel fault with a higher dip angle of 85 degree. The fault length and width are estimated to be 14 km and 13 km, respectively. Fig. 2 (right) show the bird view of the fault model for foreshock.

Tectonic stress field including the friction coefficient of the fault used in this study are mainly assumed referring to Yoshida et al. (2016) [5] and Urata et al. (2016) [9]. The maximum principle stress orientation is S69W for Hinagu fault (HF), and S83W for Futagawa fault (FF), based on the results of Yoshida et al. (2016). The variations of the Tectonic stress fields with depth is shown in Fig.3. The frictional cohesion C0 is also considered in the rupture dynamics simulations. Similar to the variations of the Tectonic stress fields with depth, the frictional cohesion C0 and the critical slip D_c are also dependent on the depth, as illustrated in Fig. 3. As shown in Fig. 3, a constant D_c of 0.4 m is applied for depths between 5 and 17 km. The frictional cohesion is 0.8 MPa at the free surface, linearly decreases to 0.2 MPa at a 5 km depth, and then remains constant. D_c and C0 is decided referring to Zhang et al. (2017) [10]. Refer to Urata et al. (2016) [9], the static and dynamic friction coefficients for Hinagu fault is 0.37 and 0.26, respectively. For Futagawa fault (FF), the static and dynamic friction coefficients is 0.39 and 0.26, respectively. Base on these parameters, the distribution of normal stress Tn, shear stress Ts and stress drop estimated on the fault plane of mainshock are shown in Fig. 4.

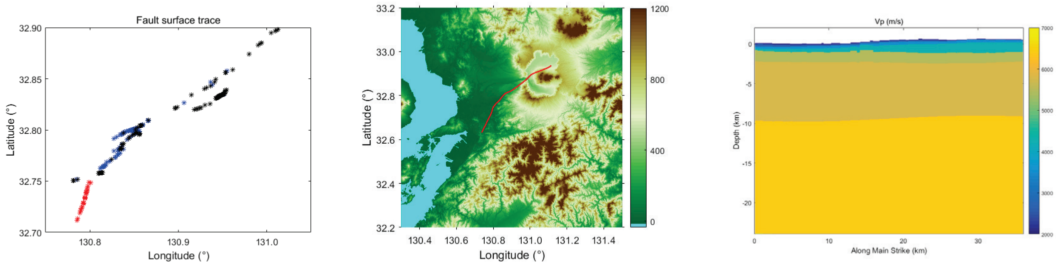

Fig. 1 –Surface rupture of the mainshock of Kumamoto earthquake (left), surface projection of the fault model (Middle) and the media along the strike of the fault model.

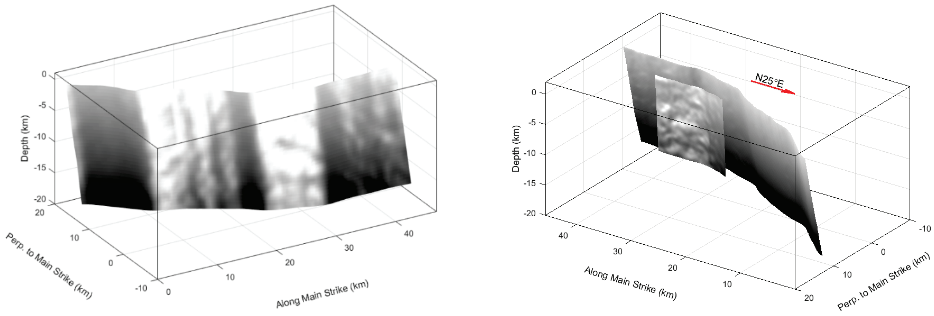

Fig. 2 – Bird views of the fault model for mainshock (left) and foreshock (right)

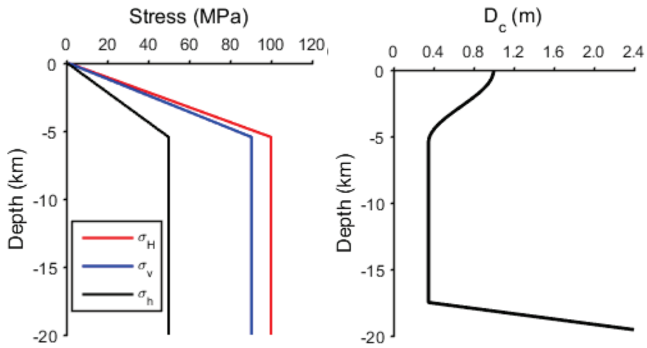

Fig. 3 – Distributions of stress fields (σ) (left), critical distance (Dc) (middle), and frictional cohesion (C0) (right)

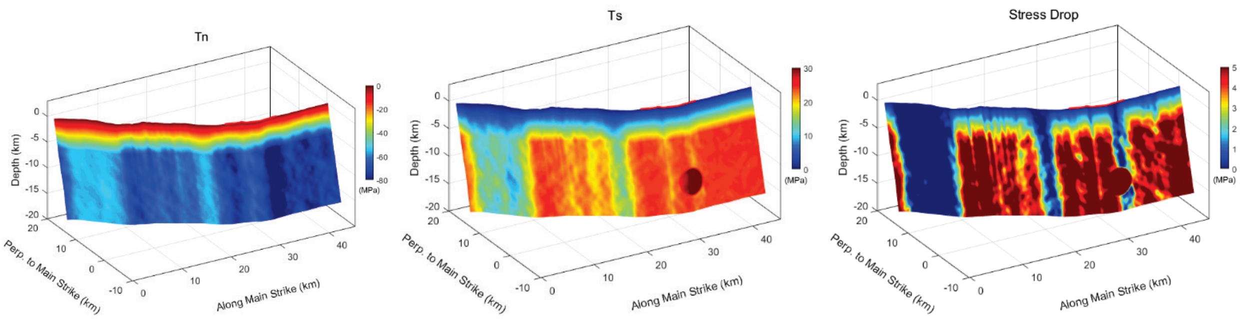

Fig. 4 – Normal stress (Tn) (left), shear stress (Ts) (middle), and stress drop (right) on the fault plane

3. Results

The mesh size of the FDM model in three directions is 50 m, the time step used in the calculation is 0.0025s, and the duration of the calculation is 20 s. The computational size for the rupture dynamics modeling is 120, 30, and 25.2 km in the three dimensions, discretized into 1200 × 300 × 252 grids. The nucleation of the dynamic rupture is a 2 km radius circular crack located on the bottom of the faults, with a depth about 12.5km. Within the nucleation patch, a relatively high stress larger (0.1%) than the fault's strength is assumed to initialize the dynamic modeling. After that, the rupture spontaneously propagates outside the unbroken area.

Fig. 5 illustrates the time contour of the fault plane every 1 s for the mainshock. The rupture time for each point is recorded when the slipping velocity first exceeds 1 mm/s. The ruptures successfully propagated from Hinagu fault (HF) to Futagawa fault (FF). Fig. 6 illustrates snapshots of the slip and the slipping rate for the mainshock, showing that the ruptures spontaneously stop at the bottom boundary of the fault plane.

The maps of the final slips for the main shock are illustrated in Fig. 6. It is clear that the rupture can propagate the entire fault plane, and the slip distribution is similar to the results of earthquake source inversion in the main features.

Fig. 7 shows an example of the comparison of observed and synthetic seismic waves at a JMA observation station of 93021 in Southern district of Kumamoto city. The figure shows the synthetic waves are generally consistent with the observed ones in the main features.

Fig. 8 shows the final slips for the fore shock. The results imply that the reason that the foreshock rupture could not propagate to the Futagawa fault is that it's triggered on the subparallel fault located southeast of the northern part of Hinagu fault, and this subparallel fault can also be interpreted from the aftershock locating.

4. Discussion

Though the synthetic seismic waves are generally consistent with the observed ones as shown in Figure 7, we try to use a realistic distribution of stress drop on fault plane to check if the results of the simulation will be changed or not. We use the method proposed by Ripperger and Mai (2004) [11] to calculate the stress drop distribution on fault plane using the final slips derived from the waveform inversion by Kobayashi et al. (2017) [7]. Fig. 9 shows the estimated stress drop distribution on seismic fault. We project the distribution of stress drop to the model used in the simulation shown in Fig. 2 (left) and do the simulation of rupture process again for the mainshock. The comparison of the observation and the newly derived synthetic waves are shown in Fig. 10. The figure shows that the revised results are also consistent with the observation in the main features.

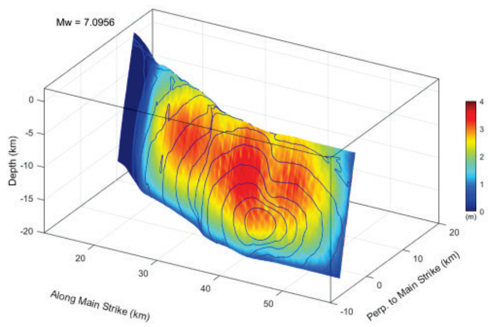

Fig. 5 – Contour for rupture propagation and the distribution of final slip on the fault for the mainshock

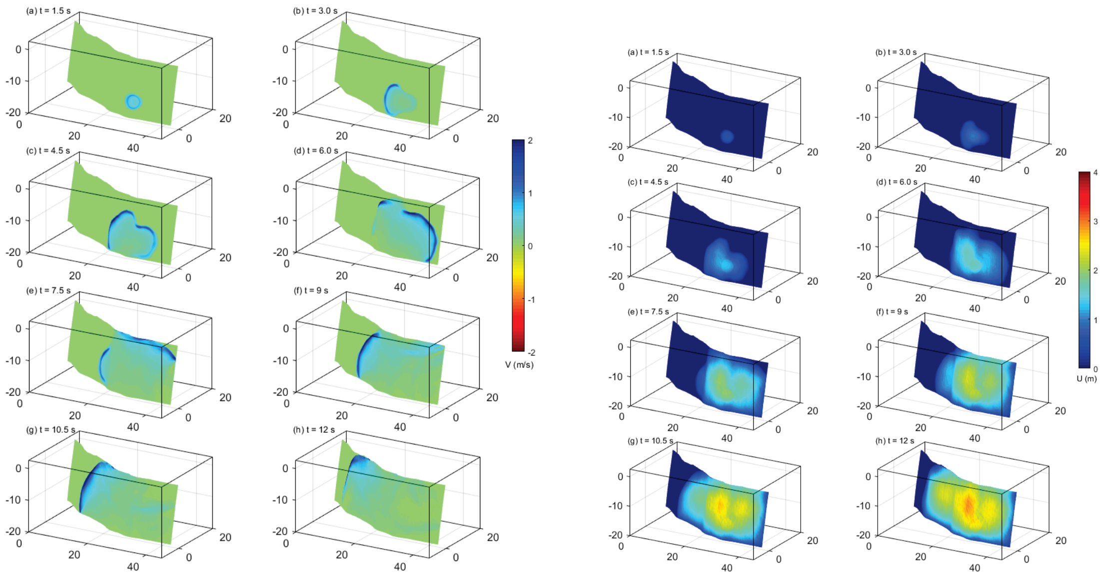

Fig. 6 – Snapshots of slipping rate (left) and slip(right) on the fault surface

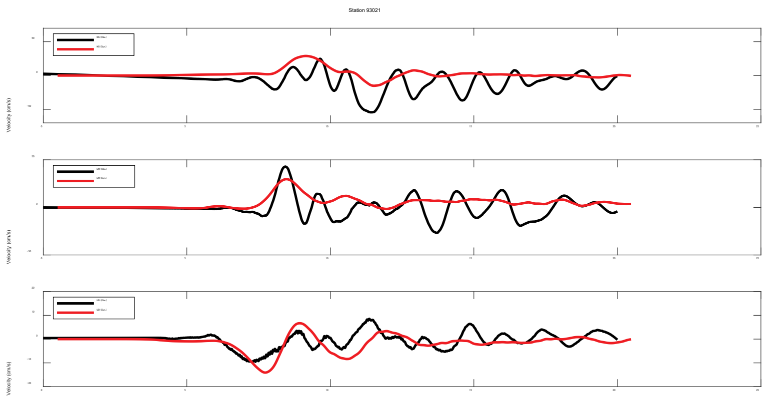

Fig. 7 – Comparison of the observed (black) and synthetic (red) seismic waves at station of 93021 in Southern district of Kumamoto city

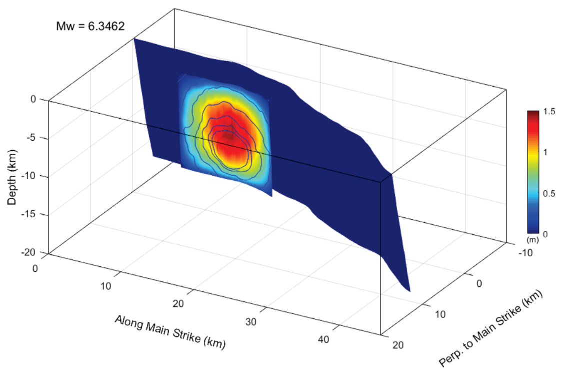

Fig. 8 – Contour for rupture propagation and the distribution of final slip on the fault for the foreshock

17th World Conference on Earthquake Engineering, 17WCEE
Sendai, Japan - September 13th to 18th 2020

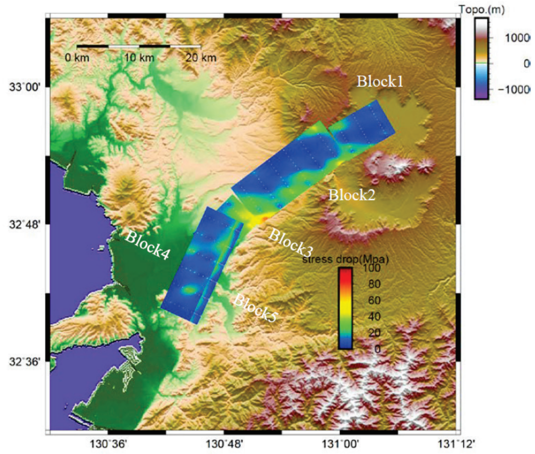

Fig. 9 – Distribution of stress drop on fault planes estimated based on the final slips derived by Kobayashi et al. (2017)

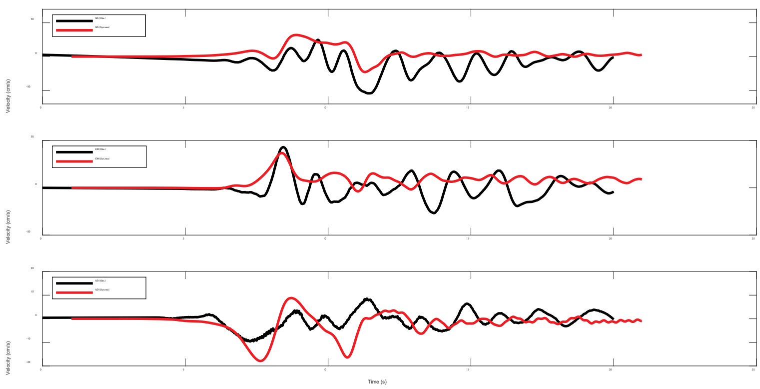

Fig. 10 – Comparison of the observed (black) and revised synthetic (red) seismic waves at station of 93021 in Southern district of Kumamoto city

5. Summary

We adopted a curved grid finite difference method (CG-FDM) [1][2] for the simulation since the method can model the complicated fault geometry for the M_w 7.0 earthquake and the seismic-wave propagation in 3D heterogeneous media. We modelled the M_w 7.0 earthquake on a smoothed non-planar fault plane based on the surface rupture trace, and also modelled the M_w 6.2 earthquake on a higher dip angle planar fault plane located in the northern part of Hinagu fault (HF). The fault planes are embedded within a 3D heterogeneous media based on the Japan integrated velocity structure model (JIVSM) proposed by Koketsu et al. (2008, 2012) [3][4]. The tectonic stress subjected to the models is estimated based on the model proposed by Yoshida et al. (2016) [5]. The dynamic friction coefficients, critical distance and the other parameters are also assumed refer to the past studies.

We performed the simultaneous dynamic rupture simulations both for the M_w 7.0 earthquake and the M_w 6.2 foreshock. For the M_w 7.0 earthquake, the rupture started from the segment of Hinagu fault (HF) and successfully propagated to the Futagawa fault (FF). For the foreshock, however, the rupture stopped on Hinagu fault (HF) and haven't propagate to the Futagawa fault (FF). The results reproduced the real rupture sequence observed during the 2016 Kumamoto earthquakes. We also confirmed that the synthetic waveforms are generally consistent with the observed ones in the main features.

6. Acknowledgements

The authors thank Professor Xiaofei Chen, Dr. Zhengguo Zhang and Mr. Houyun Yu for provide us the source code of CG-FDM, and great help in the implement of the calculation. We also thank Japan Meteorological Agency (JMA) and the National Research Institute for Earth Science and Disaster Resilience (NIED) for providing strong motion recordings.

7. References

[1] Zhang, Z., W. Zhang, and X. Chen (2014). Three dimensional curved grid finite-difference method modelling for non-planar rupture dynamics, Geophys. J. Int. 199, 860–879.

[2] Zhang, Z., H. Huang, W. Zhang, and X. Chen (2016). On the free surface problem in dynamic rupture simulation of a nonplanar fault, Bull. Seis- mol. Soc. Am. 106, 1162–1175.

[3] Koketsu, K., H. Miyake, H. Fujiwara and T. Hashimoto (2008), Progress towards a Japan integrated velocity structure model and long-period ground motion hazard map, Proc. 14th World Conf. Earthq. Eng., S10-038.

[4] Koketsu, K., H. Miyake, and H. Suzuki (2012), Japan Integrated Velocity Structure Model Version 1, Proceedings of the 15th World Conference on Earthquake Engineering, No.1773.

[5] Yoshida, K., Hasegawa, A., Saito, T., Asano, Y., Tanaka, S., Sawazaki, K., Urata, Y., Fukuyama, E., 2016, Stress rotations due to the M6.5 foreshock and M7.3 main shock in the 2016 Kumamoto, SW Japan, earthquake sequence. Geophys. Res. Lett., 43, 10097-10104.

[6] Harris, R. A., Barall, M., Aagaard, B., Ma, S., Roten, D., Olsen, K., Duan, B., Luo, B., Liu, D., Bai, K., Ampuero, J., Kaneko, Y., Gabriel, A., Duru, K., Ulrich, T., Wollherr, S., Shi, Z., Dunham, E., Bydlon, S., Zhang, Z., Chen, X., Somala, S., Pelties, C., Tago, J., Cruz-Atienza, V., Kozdon, J., Daub, E., Aslam, K., Kase, Y., Withers, K., & Dalguer, L. (2018). A suite of exercises for verifying dynamic earthquake rupture codes. Seismological Research Letters, 89(3), 1146-1162. doi: 10.1785/0220170222.

[7] Shirahama Y., Yoshimi M., Awata Y., Maruyama T., Azuma T., Miyashita Y., Mori H., Imanishi K., Takeda N., Ochi T., Otsubo M., Asahina D., Miyakawa A. (2016). Characteristics of the surface ruptures associated with the 2016 Kumamoto earthquake sequence, central Kyushu, Japan. Earth, Planets and Space, 68:191. doi:10.1186/s40623-016-0559-1.

[8] Kobayashi, H., K. Koketsu, and H. Miyake (2017). Rupture processes of the 2016 Kumamoto earthquake sequence: Causes for extreme ground motions, Geophys. Res. Lett., 44, 6002-6010, doi:10.1002/2017GL073857.

[9] Urata, Y., Yoshida, K., Fukuyama, E., & Kubo, H. (2017). 3‐D dynamic rupture simulations of the 2016 Kumamoto, Japan, earthquake. Earth, Planets and Space, 69, 150. https://doi.org/10.1186/s40623‐017‐0733‐0.

[10] Zhenguo Zhang, Wei Zhang, Xiaofei Chen, Ping'en Li, Changhua Fu; Rupture Dynamics and Ground Motion from Potential Earthquakes around Taiyuan, China. Bulletin of the Seismological Society of America ; 107 (3): 1201–1212. doi: https://doi.org/10.1785/0120160239

[11] Ripperger J, Mai PM (2004) Fast computation of static stress changes on 2D faults from final slip distributions. Geophys Res Lett 31:L18610. doi:10.1029/2004GL020594

